© 2014. Published by The Company of Biologists Ltd | Development (2014) 141, 1075-1084 doi:10.1242/dev.100123

RESEARCH ARTICLE

Eph-Ephrin signaling and focal adhesion kinase regulate actomyosin-dependent apical constriction of ciliary band cells

Oliver A. Krupke and Robert D. Burke*

ABSTRACT

Apical constriction typically accompanies inward folding of an epithelial sheet. In recent years there has been progress in understanding mechanisms of apical constriction and their contribution to morphogenetic processes. Sea urchin embryos form a specialized region of ectoderm, the ciliary band, which is a strip of epithelium, three to five cells wide, encircling the oral ectoderm and functioning in larval swimming and feeding. Ciliary band cells exhibit distinctive apical-basal elongation, have narrow apices bearing a cilium, and are planar polarized, so that cilia beat away from the mouth. Here, we show that filamentous actin and phosphorylated myosin light chain are uniquely distributed in ciliary band cells. Inhibition of myosin phosphorylation or actin polymerization perturbs this distribution and blocks apical constriction. During ciliary band formation, Sp-Ephrin and Sp-Eph expression overlap in the presumptive ciliary band. Knockdown of Sp-Eph or Sp-Ephrin, or treatment with an Eph kinase inhibitor interferes with actomyosin networks, accumulation of phosphorylated FAK (pY^{397}FAK), and apical constriction. The cytoplasmic domain of Sp-Eph, fused to GST and containing a single amino acid substitution reported as kinase dead, will pull down pY^{397}FAK from embryo lysates. As well, pY^{397}FAK colocalizes with Sp-Eph in a JNK-dependent, planar polarized manner on latitudinal apical junctions of the ciliary band and this polarization is dissociable from apical constriction. We propose that Sp-Eph and pY^{397}FAK function together in an apical complex that is necessary for remodeling actomyosin to produce centripetal forces causing apical constriction. Morphogenesis of ciliary band cells is a unique example of apical constriction in which receptor-mediated cell shape change produces a strip of specialized tissue without an accompanying folding of epithelium.

KEY WORDS: Morphogenesis, Apical constriction, Eph-ephrin signaling, Focal adhesion kinase, Planar cell polarity, Ciliary band, Sea urchin

INTRODUCTION

Apical constriction is a cellular shape change that reduces apical surface area, producing bottle-shaped cells. This process is fundamental to morphogenetic movements of cells and cellular sheets that are integral to embryogenesis. It occurs coordinately in specific cell groups and is crucial to events such as gastrulation (Sweeton et al., 1991), neurulation (Nagele and Lee, 1987) and formation of specialized epithelia (Pilot and Lecuit, 2005; Sawyer et al., 2010). The mechanisms for achieving apical constriction appear to vary between organisms and even cell types within an organism (Sawyer et al., 2010), therefore characterizing these complex regulatory mechanisms is crucial in developing a generalized understanding of morphogenesis.

It is widely accepted that actin filaments interact with myosin II motor units to provide mechanical force for apical constriction, and live imaging reveals concomitant organizational changes of actomyosin networks in apically constricting cells (Hildebrand, 2005; Lee and Harland, 2007). One of the most elaborate models for apical constriction occurs during *Drosophila* ventral furrow formation where the process is coordinated by a subcellular, ratcheting mechanism that produces a series of local, pulsed contractions in the supracellular, actomyosin meshwork; incrementally reducing apical surface area (Martin et al., 2009). Although constriction of the apical surface occurs in pulses, contraction and cortical tension within the actomyosin network occur prior to, and in the absence of, apical surface area reduction. This implies a regulatory mechanism controlling transient linkage of tensioned actomyosin networks to contact zones on the membrane surface (Roh-Johnson et al., 2012).

Echinoderm embryos have a distinctive ectodermal structure, the ciliary band. This region is a continuous, three- to five-cell wide, band of cells encircling the oral field and forming a boundary between oral and aboral ectoderm. The ciliary band, like most ectoderm, is specified in late cleavage as a consequence of TGFβ signaling (Angerer et al., 2000; Duboc et al., 2004). Nodal is expressed ventrally and establishes oral ectoderm whereas BMP2/4, also expressed ventrally, acts with BMP5/8 to specify aboral ectoderm (Lapraz et al., 2009; Ben-Tabou de Leon et al., 2013). A band of cells between the major ectoderm domains is protected from this signaling and adopts the default state of becoming ciliary band ectoderm (Saudemont et al., 2010; Bradham et al., 2009; Yaguchi et al., 2010). The presumptive ciliary band cells are distinguished by expression of Hnf6, a putative core element of the gene regulatory network that specifies ciliary band cells (Otim et al., 2004; Poustka et al., 2004). Each ciliary band cell bears a cilium and their coordinated action provides feeding and locomotory functions for the larva (Strathmann, 1971; Strathmann et al., 1972). The cilia normally beat with their power stroke directed away from the oral field (Strathmann, 2007) and are functionally polarized in the plane of the epithelium. In *Strongylocentrotus purpuratus*, the ciliary band is first apparent at ~60 hours of development (Strathmann, 1971) when cells apparently reduce their apical surface area and become bottle shaped (Burke, 1978). The mechanism of this shape change has not been explored.

The Eph receptor tyrosine kinases and their Ephrin ligands constitute the largest class of receptor tyrosine kinases in vertebrates. They are cell-surface molecules with roles in diverse biological processes, although they typically function at the interface of patterning and morphogenesis. Eph and Ephrin function in adhesion and regulate cytoskeletal organization by influencing regulatory protein complexes (Wilkinson, 2000; Klein, 2012). These include

Department of Biochemistry and Microbiology, University of Victoria, Victoria, BC V8W 3P6, Canada.

*Author for correspondence (rburke@uvic.ca)

Received 17 June 2013; Accepted 18 December 2013

Development (2014) doi:10.1242/dev.100123

interaction with focal adhesion kinase (FAK) (Carter et al., 2002), a non-receptor tyrosine kinase that regulates many cellular functions and has long been identified as a cytoskeletal regulator (Arold, 2011). Recent data identify FAK as an effector of Eph-Ephrin signaling, remodeling the cytoskeleton through recruitment and activation of Src-family kinases (Thomas et al., 1998; Parri et al., 2007; Shi et al., 2009; Darie et al., 2011).

Here, we describe ciliary band morphogenesis in the developing sea urchin embryo. The ciliary band forms in the embryonic region where ectodermal expression domains of Sp-Eph and Sp-Ephrin overlap. We show that apical constriction is independent of cell division, and loss-of-function experiments indicate that actin, myosin, Eph-Ephrin signaling and FAK are necessary for apical constriction. We propose that Eph-Ephrin signaling in the ciliary band provides a proximate cue initiating formation of a planar polarized, FAK-containing complex that regulates of apical constriction in ciliary band cells. Apical constriction of ciliary band cells is a distinctive model in which there is no inward folding of epithelium.

RESULTS

Apical surface area of ciliary band cells

The shape of ciliary band cells suggests apical constriction may be a feature of their development and we investigated whether apical surface area of ciliary band cells decreases during ciliary band formation. Between 48 and 96 hours of development, the ectoderm is transformed from a uniform sheet of cells into clearly defined regions of oral, aboral and ciliary band (Fig. 1). At 48 hours there is no measurable difference in surface area between ciliary band cells and non-ciliary band cells (Fig. 1A″,E). At 55 hours, Hnf6-positive cells have a noticeable reduction in their surface area (not shown). Over the next 17 hours the surface area of ciliary band cells is reduced by roughly one half; the majority of this occurring between 60 and 72 hours (Fig. 1A″,B″,E). Reduction in surface area is largely completed after 96 hours (Fig. 1D″). When viewed in cross section, ciliary band cells change their shape from having almost equal width and depth (Fig. 1F) to bottle-shaped (Fig. 1F′). This shape change appears to be an important event in ciliary band formation and we focused on identifying the underlying mechanism.

Change in surface area in the absence of cell division

To assess whether reduction in apical surface area of ciliary band cells is due to localized cytokinesis, we inhibited DNA polymerase at 60 hours using aphidicolin and cultured embryos in the presence of 5-ethynyl-2′-deoxyuridine (EdU) to label newly synthesized DNA and confirm inhibition of cytokinesis as an indirect effect. After 72 hours development, ciliary band cells in control embryos reduce their apical surface area (Fig. 2A′) and incorporate EdU into their nuclei (Fig. 2A), indicating DNA synthesis and subsequent cell division. Although aphidicolin completely blocks DNA synthesis (Fig. 2B) and indirectly prevents cytokinesis, ciliary band cells in treated embryos also appear to apically constrict (Fig. 2B′). Apical surface area measurements of ciliary band cells in embryos in which cell division is blocked and control embryos are not significantly different (P=0.062; Fig. 2C), indicating that reduction of apical surface area occurs independently of cytokinesis.

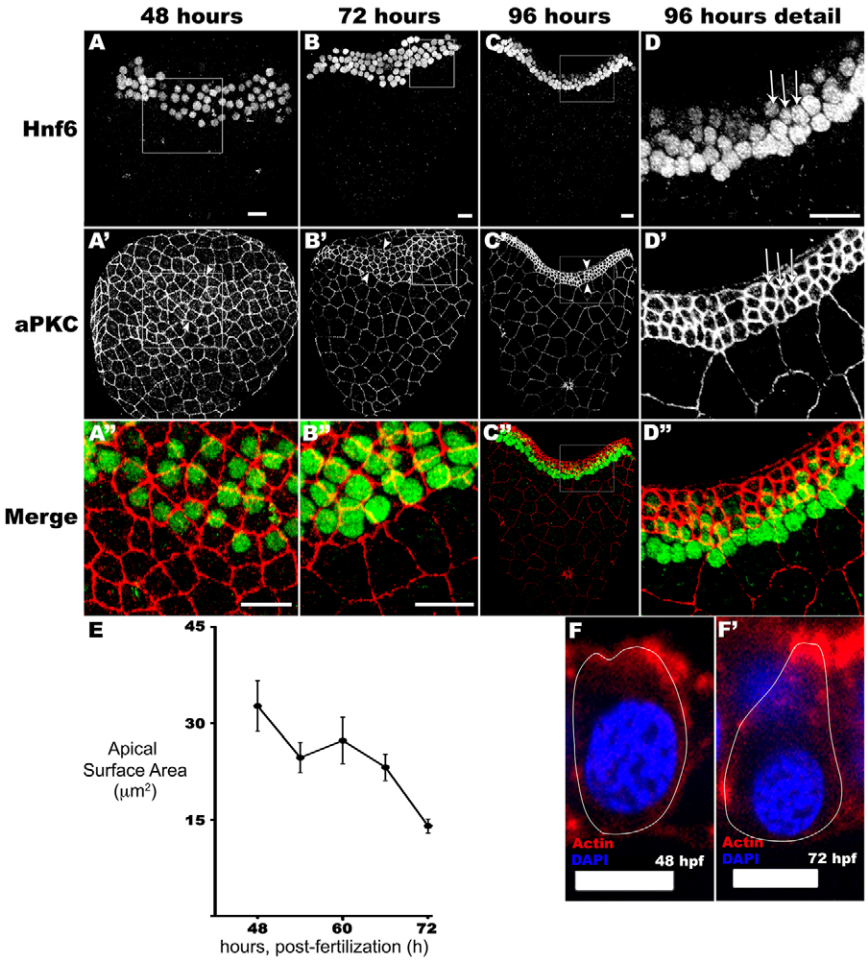

Fig. 1. Apical constriction of ciliary band cells in *S. purpuratus* during early embryonic development. (A-A″) At 48 hours, cells expressing the ciliary band marker, Hnf6 are not apically constricted compared with non-Hnf6-expressing cells. (B-B″) At 72 hours, Hnf6-expressing cells appear constricted compared with non-ciliary band cells and there is a noticeable boundary (B′, arrowheads and B″) between the ciliary band, aboral and oral ectoderm. (C-D″) At 96 hours, Hnf6-expressing cells form a band of tissue (arrowheads) with cells arranged in compact rows (arrows) that encircle the oral field. (E) Apical surface area of ciliary band cells measured from 50 to 72 hours, illustrating apical constriction (50 hours, n=1292 cells from 19 embryos; 55 hours, n=1032 cells from 16 embryos; 60 hours, n=1196 cells from 16 embryos; 65 hours, n=724 cells in ten embryos; 72 hours, n=1045 cells in 12 embryos). (F,F′) Constriction of apical cell surface (top of image) causes ciliary band cells to change their cross-sectional shape from oval at 48 hours (F) to bottle at 72 hours (F′). Scale bars: 10 μm (A-D″); 5 μm (F,F′).

Development (2014) doi:10.1242/dev.100123

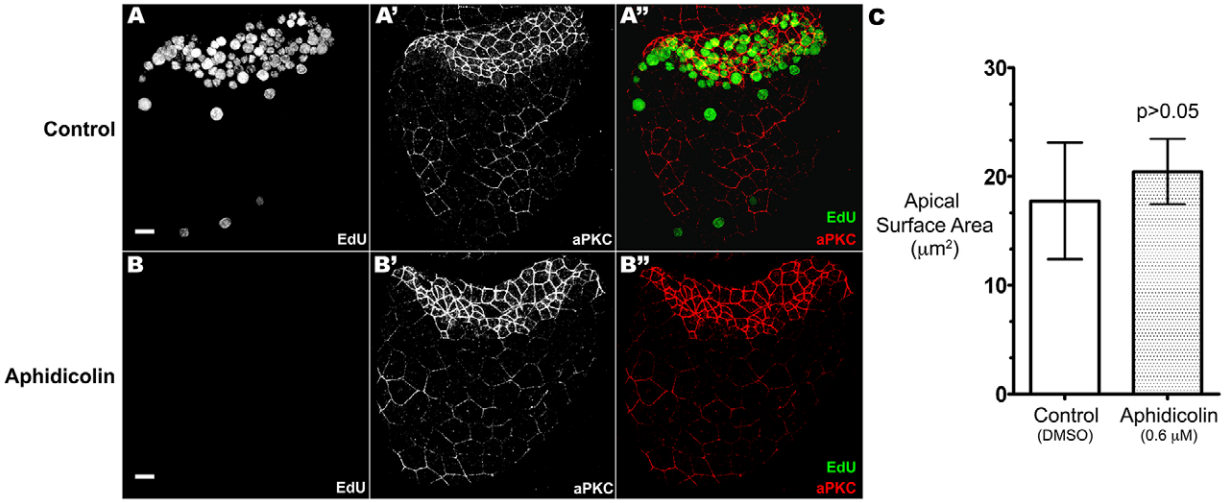

Fig. 2. Apical constriction is independent of cell division. All images are of 72 hour embryos. (A) Incorporation of EdU from 60 to 72 hours illustrates many ciliary band cells are in S phase during this interval. (A′,A″) Apical constriction is evident in untreated embryos. (B) Incorporation of EdU from 60 to 72 hours is blocked by adding 0.6 μM aphidicolin at 60 hours. (B′,B″) Apical constriction is evident in treated embryos. (C) Blocking cell division from 60-72 hours has no significant effect on apical constriction in ciliary band cells (aphidicolin, *n*=570 cells in 12 embryos; control, 1551 cells in 19 embryos). Scale bars: 10 μm.

Actin cytoskeleton of the ciliary band

At 35 hours, actin and phosphorylated myosin light chain (pS[19]MLC) are distributed uniformly around the apical margin of ciliary band cells and colocalize with apical junction components (Fig. 3A-A‴). Beginning at about 40 hours, actin and pS[19]MLC are not associated solely with cell junctions (Fig. 3B-B″) but are distributed throughout the apical cortex of ciliary band cells. At 72 hours, pS[19]MLC is in discontinuous patches at the cell periphery and actin is dispersed in strands and patches in the apical cortex of ciliary band cells (Fig. 3C-C″). This rearrangement suggests a role during apical surface area reduction in ciliary band cells.

We hypothesized that the actomyosin network provides some of the mechanical force that contributes to apical constriction and that interfering with actomyosin contractility would lead to a loss of apical constriction in ciliary band cells. We tested this using cytochalasin D (Miyoshi et al., 2006) to disrupt actin filaments (Fig. 4A-A″), or ML 7 (Uehara et al., 2008) to inhibit myosin light chain kinase (Fig. 4B-B″). Cytochalasin D-treated embryos are rounded with loosely packed cells expressing Hnf6 (Fig. 4A) and distribution of actin and pS[19]MLC are perturbed (Fig. 4A′,A″). Specifically, pS[19]MLC occurs in circular structures in the ciliary band (Fig. 4A′, arrows and inset). Similarly, actin networks in the ciliary band are discontinuous and appear as hollow circles (Fig. 4A″, arrows and inset). Embryos treated with ML 7 are rounded and Hnf6-expressing cells are loosely packed (Fig. 4B). Latitudinal distribution of pS[19]Myo is irregular (Fig. 4B′, arrowheads and inset). Similarly, actin networks are irregular and

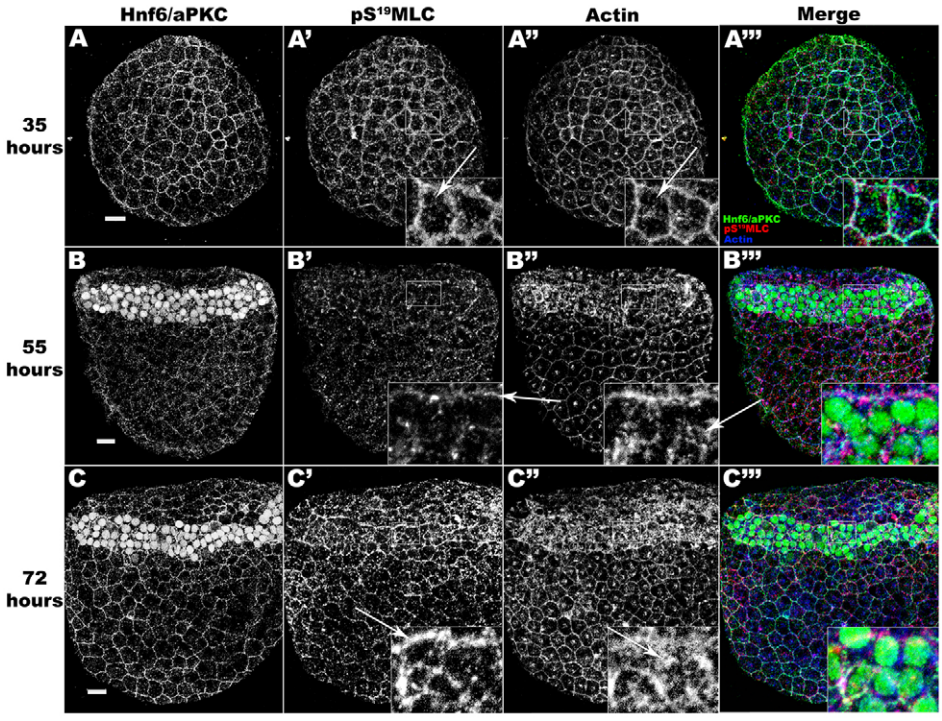

Fig. 3. Cytoskeletal networks of actin and phospho-myosin (pS[19]MLC) undergo remodeling in ciliary band cells during apical constriction with no apparent changes in actomyosin of non-ciliary band cells. (A) At 35 hours, cell junctions are clear and Hnf6 is not yet expressed. (A′,A″) pS[19]MLC and actin localize primarily to apical junctions, with minimal amounts in the apical cortex (inset, arrows). (B) At 55 hours, presumptive ciliary band cells express Hnf6 and cell junctions are indicated with anti-aPKC antibody. (B′) The polarized distribution of pS[19]MLC is evident on latitudinal membranes of the ciliary band (inset, arrow). (B″) Ciliary band-specific remodeling of actin is evident in the apical cortex (inset, arrow). (C) At 72 hours, ciliary band cells have constricted apically. (C′) A continuous, supracellular network of pS[19]MLC is present in the ciliary band, characterized by polarized expression on latitudinal junctions (inset, arrow). (C″) Continuous actin filaments form a supracellular network in the ciliary band accompanied by formation of dense actin networks in apical cortices of ciliary band cells (inset, arrow). Scale bars: 10 μm.

Development (2014) doi:10.1242/dev.100123

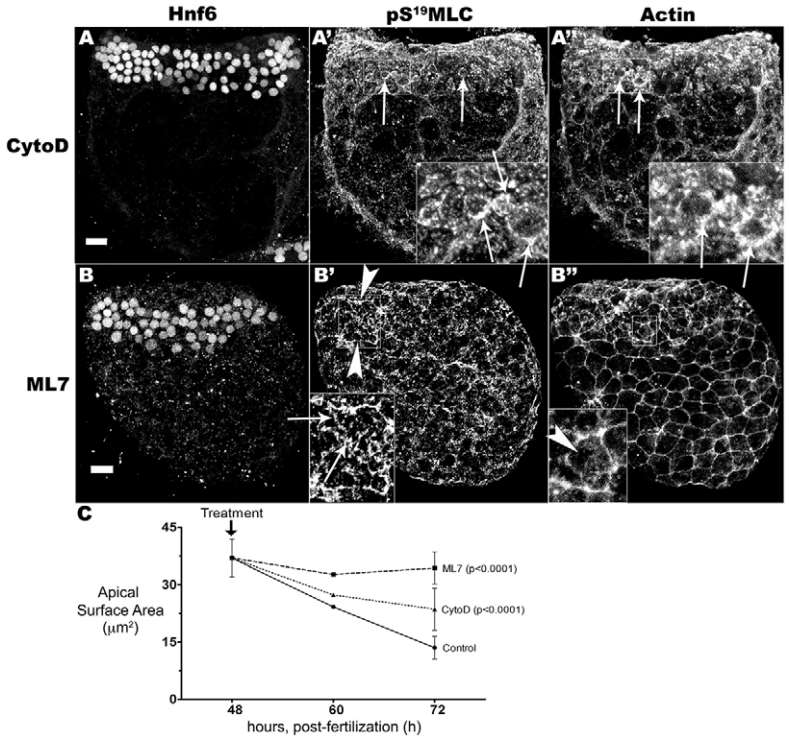

Fig. 4. Treatment with cytochalasin D or ML 7 disrupts cytoskeletal networks of actin and phospho-myosin (pS[19]MLC) and inhibits apical constriction. All images are of 72 hour embryos. (A-A″) Embryos exposed to 20 μM cytochalasin D at 48 hours fail to form a ciliary band and form rounded embryos that lack a clearly defined ciliary band. (A) Ciliary band cells are loosely packed. (A′) Random accumulations of pS[19]MLC appear on apical junctions of ciliary band cells (inset, arrows). (A″) Patchy actin is distributed randomly on all cell junctions throughout the ciliary band (inset, arrows). (B-B″) Treatment with 5 μM ML 7 at 48 hours disrupts ciliary band formation. (B) Embryos are ovoid and lack a clearly defined ciliary band. (B′) Distribution of pS[19]MLC is polarized to latitudinal membranes in some areas of the ciliary band (arrowheads). Aberrant, pS[19]MLC-containing structures form in the apical cortices of cells (inset, arrow). (B″) Dense actin networks are present in only some areas of the ciliary band and actin does not accumulate in apical cortices (inset, arrowhead). (C) Inhibitors of actin polymerization and myosin light chain kinase block apical constriction of ciliary band cells. Apical surface area of ciliary band cells in control embryos is reduced more than 50% from 48 to 72 hours (solid line; 48 hours, *n*=625 cells in ten embryos; 60 hours, *n*=747 cells in ten embryos; 72 hours, *n*=788 cells in ten embryos). Apical constriction is significantly reduced in ciliary band cells of embryos treated with the cytoskeletal inhibitor cytochalasin D (dotted line; 48 hours, *n*=625 cells in ten embryos; 60 hours, *n*=637 cells in ten embryos; 72 hours, *n*=639 cells in ten embryos) or ML-7 (dashed line; 48 hours, *n*=625 cells in ten embryos; 60 hours, *n*=654 cells in ten embryos; 72 hours, *n*=597 cells in ten embryos). Scale bars: 10 μm.

discontinuous in these embryos (Fig. 4B″) and apical cortices often lack actin accumulation. As can be seen from Fig. 4C ciliary band cells in embryos treated with ML 7 (dashed line) or cytochalasin D (dotted line) are less apically constricted than those of control embryos (solid line). This indicates polymerization of actin filaments and phosphorylation of myosin light chain are necessary for apical constriction of ciliary band cells.

Ectodermal expression of Sp-Eph and Sp-Ephrin and interaction with FAK

Preliminary data indicated that Sp-Eph and Sp-Ephrin were expressed in ectoderm beginning at gastrulation. Further analysis using antibodies against pY[379]Eph and Sp-Eph indicated that Sp-Eph is expressed throughout the oral and ciliary band ectoderm (Fig. 5E,F) and becomes phosphorylated in the ciliary band during apical constriction (Fig. 5A-B″; ciliary band boundary to oral ectoderm marked by arrowheads, boundary to aboral ectoderm marked by arrows). In the ciliary band, beginning at 48 hours, Sp-Eph is polarized in its distribution; it is most abundant on latitudinal membranes (Fig. 5E,F, arrows). This contrasts with the expression in the oral ectoderm, where Sp-Eph is expressed uniformly around the periphery of cells (Fig. 5F, asterisks). Antibodies against Sp-Ephrin indicate that the protein is expressed on aboral ectoderm and the ciliary band (Fig. 5A,A′,B,B′). Expression of Sp-Ephrin could not be detected in the oral ectoderm during ciliary band formation (Fig. 5B,B′). The overlapping expression of Sp-Eph and Sp-Ephrin in the region in which the ciliary band is forming and the detection of the phosphorylated form of the Sp-Eph receptor suggests that Sp-Eph is signaling in presumptive ciliary band cells. A ciliary band expression pattern similar to that of Sp-Eph is observed using pY[397]FAK antibody (Fig. 5C,E′,F′), and these colocalize during apical constriction (Fig. 5E″,F″) suggesting an interaction.

Following these observations, we investigated interactions between Sp-Eph and pY[397]FAK *in vitro* using a GST-tagged, cytoplasmic domain (322-762) of native Sp-Eph (Fig. 5D). This protein failed to reliably pull down pY[397]FAK in epithelial cell lysate from 72-hour embryos (Fig. 5D, lower panel). Because kinase domains often bind substrates transiently, releasing them upon phosphorylation, we created a kinase-dead form of this construct as a substrate trap (Roose et al., 2005) and we found it pulls down pY[397]FAK (Fig. 5D, top panel). This indicates a potential physical interaction between Sp-Eph and pY[397]FAK in ciliary band cells.

Eph-Ephrin signaling is necessary for apical constriction

To assess the role of Eph-Ephrin signaling during apical constriction, we blocked translation of Sp-Eph or Sp-Ephrin in the embryo by morpholino-substituted antisense oligonucleotide (MASO) injection (Fig. 6). For each protein, we injected two, non-overlapping oligonucleotides to knock down expression with 42.4% (±16.4% s.e.m.) mean knockdown based on fluorescence intensity. When we knocked down Sp-Eph or Sp-Ephrin, a distinct ciliary band failed to form after 72 hours and embryos were ovoid in shape (Fig. 6A-B′). At 72 hours, actin and pS[19]MLC in Sp-Eph knockdown embryos appear in circular or crescent-shaped patches throughout the ciliary band (Fig. 6C-C‴). These patches appear restricted to individual cells for pS[19]MLC (Fig. 6C′, arrow and inset) and for actin (Fig. 6C″, arrow and inset) and do not form an interconnected, supracellular network as seen in untreated embryos (Fig. 3), indicating Sp-Eph is necessary for actomyosin reorganization during ciliary band formation. Furthermore, ciliary band cells in MASO-injected embryos appear larger than in control embryos (Fig. 6D-F) and when we quantified apical surface area, we found apical constriction is significantly reduced in knockdown embryos ($P<0.0001$; Fig. 6G), indicating Sp-Eph and Sp-Ephrin are necessary for apical constriction of ciliary band cells.

Ciliary band-specific accumulation of pY[397]FAK is regulated by Eph-Ephrin signaling

We investigated whether ciliary-band-specific FAK phosphorylation is dependent on Eph-Ephrin signaling (Fig. 7). Prior to ciliary band

Development (2014) doi:10.1242/dev.100123

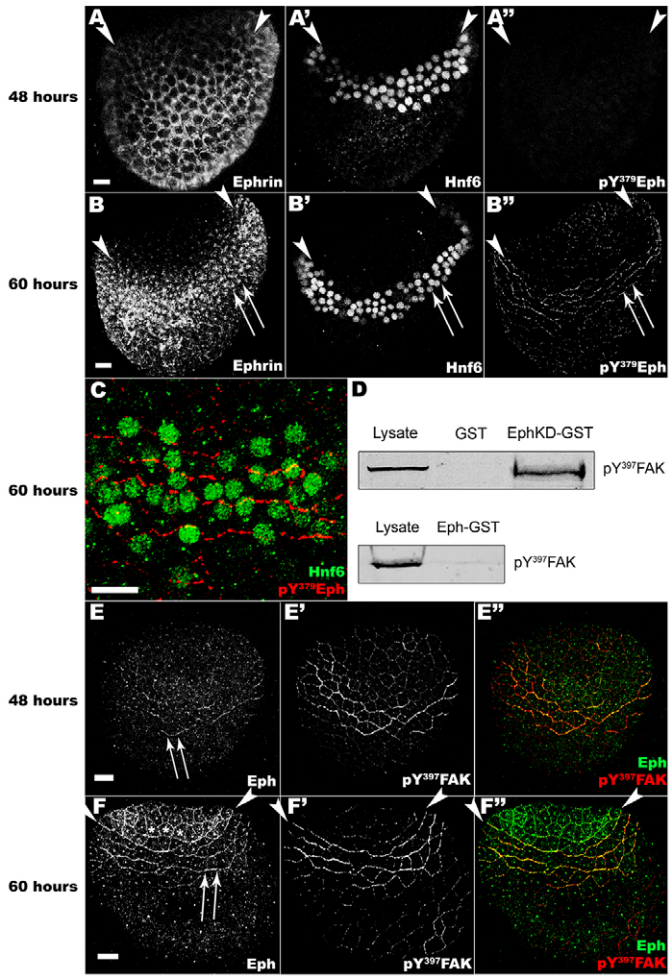

Fig. 5. During apical constriction, Eph and Ephrin expression overlap in the ciliary band and Eph becomes phosphorylated along latitudinal membranes where it colocalizes with pY^{397}FAK. Antigens and developmental stages are indicated. Arrowheads mark oral ectoderm-ciliary band boundary; arrows mark aboral ectoderm-ciliary band boundary. (A-A′) Region-specific expression of Sp-Ephrin prior to apical constriction. (A) Sp-Ephrin is primarily on aboral and ciliary band ectoderm. (A′) Expression of Hnf6 marks the ciliary band. (A″) Prior to apical constriction, pY^{379}Eph is not detected. (B-B″) Ciliary band-specific colocalization of pY^{379}Eph and Sp-Ephrin during apical constriction. (B) Ephrin expression is restricted to aboral and ciliary band ectoderm. (B′) Hnf6 expression indicates ciliary band cells are forming a tightly packed band of tissue. (B″) pY^{379}Eph is detected on junctions in the ciliary band and largely absent from oral and aboral ectoderm. (C) During apical constriction, pY^{379}Eph is polarized to latitudinal membrane junctions of ciliary band cells. (D) Sp-Eph cytoplasmic domain and pY^{397}FAK interact physically. (Top panel) A GST fusion protein of kinase-dead Sp-Eph (EphKD) cytoplasmic domain acts as a substrate trap, showing a specific interaction with pY^{397}FAK in an ectodermal cell lysate from *S. purpuratus* embryos at 72 hours. (Bottom panel) A native form of Eph cytoplasmic domain does not reliably pull down detectable quantities of pY^{397}FAK from an ectodermal lysate. (E-E″) Prior to apical constriction, Sp-Eph and pY^{397}FAK are apparent in the presumptive ciliary band. (E) Sp-Eph is apparent on apical junctions within oral and ciliary band ectoderm, and latitudinal polarization is evident on junctions bordering the aboral ectoderm (arrows). (E′) pY^{397}FAK becomes abundant on apical junctions in the ciliary band where it colocalizes (E″) with Sp-Eph. (F-F″) Distinct latitudinal polarization of Sp-Eph and pY^{397}FAK during apical constriction of ciliary band cells. (F) Sp-Eph distribution is polarized in the ciliary band and does not extend into aboral ectoderm (arrows) but is uniformly distributed on junctions of oral ectoderm (asterisks). (F′) Polarized expression of pY^{397}FAK is restricted to the ciliary band where it colocalizes with Eph (F″). Puncta in E and F appear to represent recognition of material within the basal body of each cell in the embryo. Scale bars: 10 µm.

specification, pY^{397}FAK is uniformly distributed on cell membranes (Fig. 7A) and polarized accumulation begins in the presumptive ciliary band (Fig. 7B). Accumulation of pY^{397}FAK at latitudinal junctions of the ciliary band continues throughout apical constriction (Fig. 7C,D). Knockdown of Sp-Eph or Sp-Ephrin expression causes a distinct reduction of pY^{397}FAK accumulation in the ciliary band (Fig. 7E,F). Using quantitative confocal microscopy, we identified that the relative abundance of pY^{397}FAK in the ciliary band at 60 hours is 3.25 times more than in aboral ectoderm (Fig. 7G). When we perturb Eph-Ephrin signaling by MASO-induced knockdown or inhibition of Sp-Eph kinase, pY^{397}FAK abundance is reduced to less than twofold that of aboral ectoderm (Fig. 7G). Thus, Eph-Ephrin signaling is necessary for pY^{397}FAK accumulation. A similar effect is achieved using PF573 (Fig. 7G, right bar), a small molecule inhibitor that obstructs the ATP-binding pocket of FAK (Slack-Davis et al., 2007). These data indicate Eph-Ephrin signaling regulates pY^{397}FAK accumulation in ciliary band cells during apical constriction.

Apical constriction requires Eph-Ephrin signaling and phosphorylation of FAK

By adding specific inhibitors and measuring apical surface area, we further assessed the roles of Eph-Ephrin signaling and FAK catalytic activity on apical constriction of ciliary band cells (Fig. 8). In the presence of NVP (1.75 µM), an Eph kinase inhibitor, ciliary band formation and accumulation of pY^{397}FAK are disrupted (Fig. 8B), and apical surface area of ciliary band cells does not change (Fig. 8D), indicating a lack of apical constriction. To determine the role of pY^{397}FAK, we used PF573 to block phosphorylation of Y397 and we measured the effect in ciliary band cells. Apical constriction is blocked by PF573 (10 µM; Fig. 8C,D), indicating that FAK phosphorylation on Y397 is crucial. These data support a model in which forward Eph-Ephrin signaling regulates apical constriction of the ciliary band cells through pY^{397}FAK.

Planar cell polarity in ciliary band cells

Using an inhibitor specific to the non-canonical Wnt pathway, we investigated the role of planar cell polarity in the ciliary band (Fig. 9). We treated embryos with a cell permeant, c-Jun N-terminal peptide (Range et al., 2013) and examined polarization of pY^{397}FAK or pY^{379}Eph in ciliary band cells (Fig. 9A-B′). In control embryos, the abundance of pY^{397}FAK on latitudinal junctions of the ciliary band is 12.21 times greater than on longitudinal junctions when measured by normalized fluorescence intensity (Fig. 9A). When treated with JNK inhibitor, the abundance of pY^{397}FAK is equal on latitudinal junctions is significantly reduced (P<0.001) to 1.02 times (nearly equal) the amount on longitudinal junctions (Fig 9A′). Similarly, polarization of Y^{397}Eph to latitudinal membranes is significantly reduced (3.28 times greater in controls versus 2.27 times greater in treated embryos; P<0.001) when JNK is inhibited (Fig. 9B,B′), indicating polarization of these signaling molecules in the ciliary band is dependent on the non-canonical Wnt pathway. Interestingly, when we quantify apical surface area of ciliary band cells in these JNK-treated embryos and compare them with control cells, there is no significant difference (P=0.303; Fig. 9C), implying that the mechanisms driving apical constriction and polarization of pY^{379}Eph and pY^{397}FAK are independent (Fig. 9D).

DISCUSSION

Our data support a model in which Eph-Ephrin forward signaling initiates formation of a planar-polarized, pY^{397}FAK-containing, signaling complex that regulates actomyosin-mediated

Development (2014) doi:10.1242/dev.100123

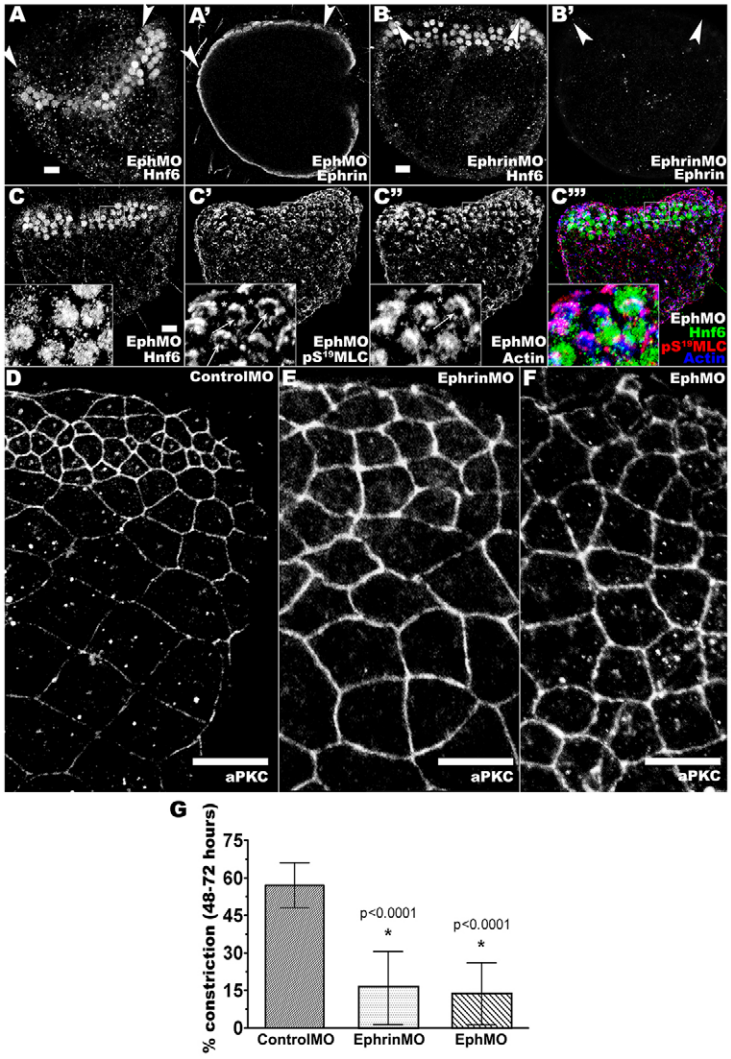

Fig. 6. Blocking Eph-Ephrin signaling prevents apical constriction and formation of supracellular networks in the ciliary band. Arrowheads mark the boundary between oral and ciliary band ectoderm. All images are of 72 hour embryos. (A,A′) Knockdown of Sp-Eph expression by morpholino injection (EphMO – 250 µM solution) produces rounded embryos. (A) Hnf6 expression indicates loosely packed ciliary band cells. (A′) Sp-Ephrin expression extends into the oral ectoderm. (B,B′) Knockdown of Sp-Ephrin expression by morpholino injection (EphrinMO – 200 µM solution) produces rounded embryos. (B) Hnf6 expression indicates loosely packed ciliary band cells. (B′) Sp-Ephrin expression is faint in aboral ectoderm and absent in oral ectoderm. (C-C‴) Sp-Eph knockdown disrupts the supracellular actomyosin network in the ciliary band. (C) The ciliary band is loosely packed and Hnf6 marks individual cells. (C′,C″) pS^{19}MLC and actin in the ciliary band form discrete, hollow circles (inset, arrows), closely associated with apical membranes of individual cells. Gaps are present between adjacent cells (inset, asterisks), indicating a discontinuous actomyosin network. (C‴) Merged channels illustrate individual cells and associated actomyosin meshwork with gaps between cells and absence of a supracellular network. (D) Ciliary band cells in control embryos constrict normally and form a tightly packed row, three to five cells wide. (E,F) Morpholino-induced knockdown of Sp-Ephrin (E) or Sp-Eph (F) disrupts apical constriction and an organized ciliary band is not formed. (G) Apical constriction of ciliary band cells is significantly reduced in Sp-Eph and Sp-Ephrin knockdown embryos. Percentage constriction=(apical surface area at 72 hours/apical surface area at 48 hours)×100. Control, *n*=795 cells in nine embryos; EphMO, *n*=625 cells in ten embryos; EphrinMO, *n*=792 cells in 11 embryos. The mean knockdown efficiency for MASO injections based on fluorescence intensity was 42.4%. Scale bars: 10 µm.

contractility, producing apical constriction. The overlap of Sp-Eph and Sp-Ephrin expression appears to activate Sp-Eph within the presumptive ciliary band. A number of studies describe effects on FAK following Ephrin stimulation of Eph. These include increased autophosphorylation on Y^{397} with downstream effects on cytoskeletal reorganization and cell shape (Shi et al., 2009; Moeller et al., 2006; Carter et al., 2002; Ohashi et al., 2000). There appears to be a role for FAK during ciliary band morphogenesis; its catalytic activity is necessary for apical constriction, pY^{397}FAK accumulates specifically on latitudinal, ciliary band membranes and Eph-Ephrin signaling is necessary for this accumulation. Furthermore, colocalization of pY^{397}FAK and Sp-Eph on latitudinal membranes of the ciliary band and the putative molecular interaction emphasize a close functional relationship. We propose Sp-Eph and FAK act in an apical complex; regulating assembly of cytoskeletal networks necessary for transducing centripetal forces that reduce apical size during ciliary band morphogenesis (Fig. 9E). There are a number of potential mechanisms by which FAK activation can function in the regulation of actin-mediated contractility. These include transduction through Src family kinases, guanine nucleotide exchange factors, GTPase-activating proteins and Rho-family GTPases (Thomas et al., 1998; Tilghman and Parsons, 2008; Burridge and Wennerberg, 2004). This provides a potential mechanism whereby extracellular Sp-Ephrin elicits a receptor-mediated (Sp-Eph) response to change cell shape.

Loss-of-function experiments show filamentous actin and myosin light chain kinase are necessary for apical constriction, and rearrangements in their distribution occur immediately prior to shape change. The observed distribution is not consistent with a purse string model in which a circumferential band of actin in each cell is predicted. Rather, our observations are consistent with a model of apical constriction, where centripetal force is produced by contractions of the actomyosin network at the medial apical cortex (Martin et al., 2009). Furthermore, when we block apical constriction by perturbing Eph-Ephrin signaling, we also disrupt supracellular cytoskeletal networks in the ciliary band, illustrating that Eph-Ephrin signaling is involved in remodeling actomyosin networks during apical constriction of ciliary band cells (Fig. 9E).

Ciliary band cells are polarized within the epithelial plane and this is apparent functionally; cilia have their power stroke oriented away from the oral field (Strathmann, 2007). Sp-Eph and pY^{397}FAK exhibit a polarized distribution and Eph-Ephrin signaling and FAK catalytic activity do not appear to initiate polarization, as loss of function interferes with the extent of immunoreactivity of polarized components without noticeably altering their distribution. By contrast, inhibition of JNK leads to a loss in polarization of pY^{397}FAK and pY^{379}Eph with no apparent effects on the level of immunoreactivity

Development (2014) doi:10.1242/dev.100123

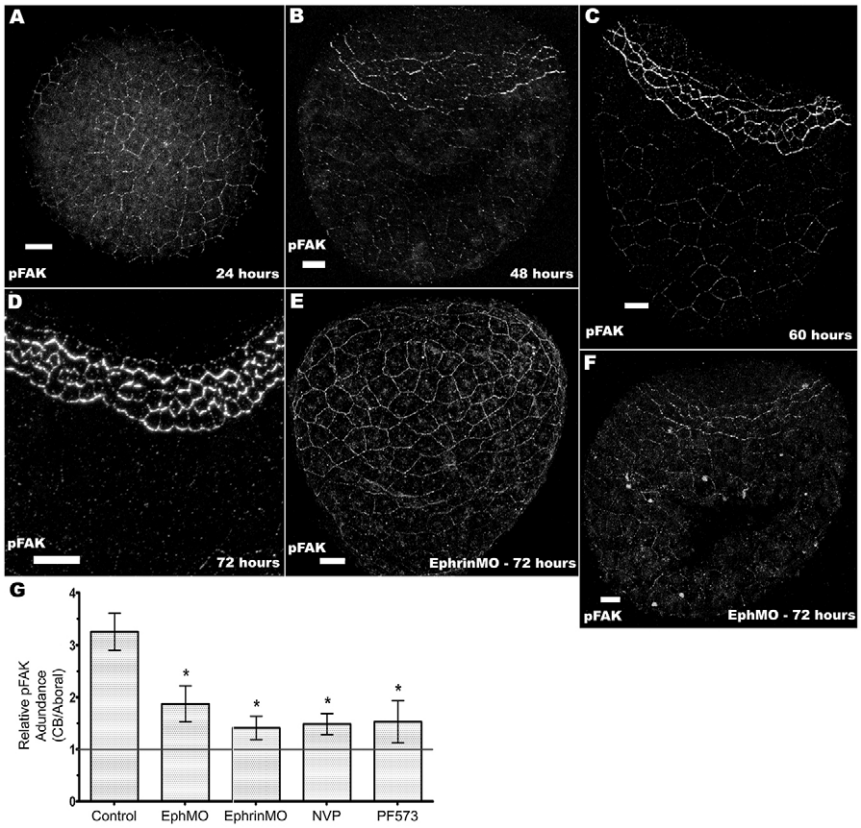

Fig. 7. Ephrin signaling through Eph is necessary for phosphorylation of focal adhesion kinase during ciliary band formation. (A) pY^{397}FAK is uniformly distributed on cell-cell junctions at 24 hours. (B) At the onset of apical constriction, pY^{397}FAK accumulates on latitudinal junctions in the ciliary band. (C,D) pY^{397}FAK intensity on latitudinal junctions in the ciliary band increases as apical constriction continues (C) and the fully formed ciliary band (D) shows abundant pY^{397}FAK. (E,F) Knocking down Sp-Ephrin (E; EphrinMO – 200 µM solution) or Sp-Eph (F; EphMO – 250 µM solution) expression disrupts pY^{397}FAK accumulation in the ciliary band. (G) Blocking Eph-Ephrin signaling or FAK catalytic activity significantly reduces relative abundance of pY^{397}FAK (*denotes P<0.001). In control treatments relative pY^{397}FAK abundance in the ciliary band is >3.2 (left bar). Injection of Eph or Ephrin morpholino (as above) or addition of Eph kinase inhibitor (NVP) at 1.75 µM, results in a significant loss in pY^{397}FAK accumulation. A similar response is achieved by adding 10 µM of PF573, an inhibitor specific to pY^{397}FAK (right bar). Relative abundance is measured by comparing fluorescence intensity of pixels within the ciliary band to those within aboral ectoderm at 60 hours. A relative abundance value of 1 is equivalent to the abundance of pY^{397}FAK on aboral ectoderm. All pixels in the aboral and/or ciliary band ectoderm were quantified for each embryo. Untreated, n=10 embryos; EphMO, n=12 embryos; EphrinMO, n=11 embryos; Eph inhibitor, n=10 embryos; pFAK inhibitor, n=14 embryos. Mean knockdown efficiency for all MASO injections based on fluorescence intensity was 42.4%. Scale bars: 10 µm.

and no significant loss of apical constriction. We speculate that the non-canonical, Wnt planar cell polarity pathway is responsible for directing assembly of an actomyosin-regulating, Sp-Eph/FAK complex specifically along latitudinal junctions within the ciliary band. Furthermore, polarity and apical constriction appear to be dissociable phenomena that are regulated independently (Fig. 9D,E).

In widely studied models of apical constriction, reduction of apical surface area is followed by inward folding of epithelium and although additional morphogenetic forces and planar cell polarity have been implicated in the folding process, individual contributions have not been resolved (Sawyer et al., 2010; Nishimura et al., 2012). Ciliary band formation is a unique example of morphogenesis because there is no accompanying, large-scale, inward flexion of adjacent ectoderm; rather cells change shape producing a tightly packed array of cilia with modest outward flexion. This indicates that apical constriction does not function independently to produce large-scale morphogenetic movements. The apical constriction of ciliary band cells is informative in that it indicates participation of adjacent tissues in morphogenetic folding. The nature of the coupling of apical constricting and adjacent tissues remains a key feature in the development of models that seek to describe the complex mechanisms linking patterning to the mechanical forces that drive morphogenesis.

MATERIALS AND METHODS

Embryo culture and injection

Eggs and sperm were collected from *S. purpuratus* adults induced to spawn with 0.55 M KCl or by shaking or gentle prodding. Sperm was diluted 1:1000 in filtered seawater prior to fertilization and embryos were grown at 14°C. Unless otherwise mentioned, inhibitors were added 48 hours postfertilization. Eggs were prepared for microinjection as described previously (Krupke et al., 2013). Injection solutions containing 22.5% glycerol, either RhodamineB-dextran (Sigma, R9379) or Fluorescein isothiocyanate-dextran (Sigma, 46945) and RNA were microfiltered at 5000 ***g*** for 1 minute using 0.22 µm Ultrafree centrifugal filters (Millipore). Morpholino antisense oligonucleotides were obtained from GeneTools and injected as previously described (Krupke et al., 2013).

Plasmids and reagents

Oligonucleotide DNA primers were obtained from Operon. Sequences encoding full-length Sp-Ephrin and Sp-Eph were obtained by PCR from cDNA isolated from 72 hour *S. purpuratus* embryos and cloned using standard methods. Morpholino antisense oligonucleotides were obtained from GeneTools. EphrinMO1: 5′-AAATTTAGTCCTGGAAAGATG-AGAC-3′. EphrinMO2: 5′-CTCCAGGGTCAAAGTGCTCAGGTAT-3′. EphMO1: 5′-ATTGGAAAGAGTAAATCCGAGATGT-3′. EphMO2: 5′AAATAAGTCATTCTCTCCTCTCCGT-3′. ControlMO: 5′-GAATGA-AACTGTCCTTATCCATCA-3′. Inhibitors (Tocris Biosciences) were used as follows: 50 µM c-Jun peptide (cat. no. 1989), 20 µM cytochalasin D (cat. no. 1233), 5 µM ML 7 (cat. no. 4310), 1.75 µM NVP BHG 712 (NVP, cat. no. 4405), 10 µM PF 573228 (PF573, cat. no. 3239).

Antibody production

Proteins were produced using pET28a vector (Novagen) for expression of 6×His-tagged proteins. The C-terminal half of Sp-Eph [amino acids (aa) 447-746] and the N-terminus of Sp-Ephrin (aa 28-169) were amplified by PCR, cloned into pET28a and protein expression was induced in *E. coli* using standard protocols. Bacterial lysate was prepared using BugBuster (Novagen) and protein was solubilized in binding buffer (6 M guanidine HCl, 0.5 M NaCl, 100 mM Na_2HPO_4, 100 mM NaH_2PO_4, 10 mM imidazole, 10 mM Tris, 1 mM 2-mercaptoethanol, pH 8.0) prior to affinity purification by immobilized metal ion affinity chromatography (IMAC) using Chelex 100 Resin (Bio-Rad). Proteins were purified by size exclusion on a Hi Load 16/60 Superdex 75 prep grade column (GE Healthcare) using the ÄKTAprime plus system (GE Healthcare). Purified protein was concentrated and dialyzed in PBS and mixed with Freund's complete adjuvant (Sigma) for initial immunization or with Freund's incomplete

Development (2014) doi:10.1242/dev.100123

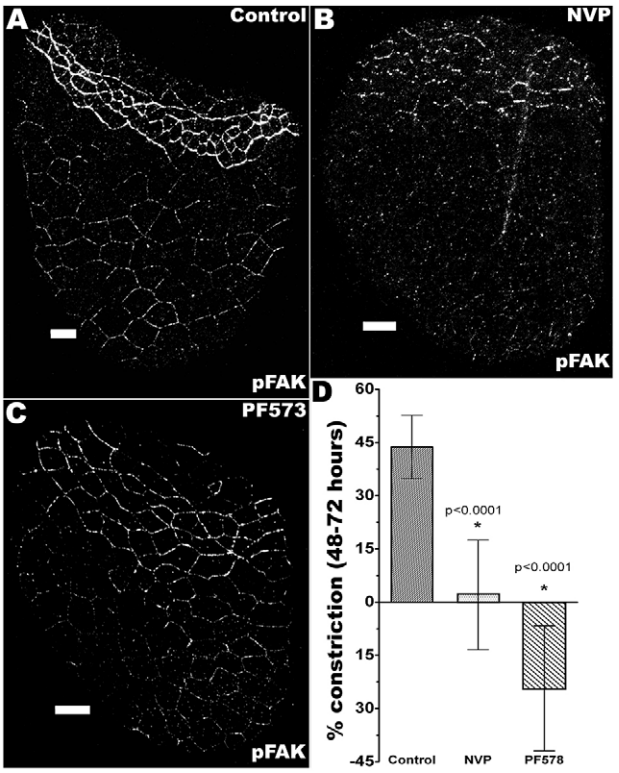

Fig. 8. Phosphorylation of focal adhesion kinase and forward signaling through Eph are necessary for apical constriction of ciliary band cells. Antigens and treatments are indicated. All images are of 72 hour embryos. (A) Control embryos accumulate pY[397]FAK at apical membrane junctions within the ciliary band. (B) Blocking Eph kinase (NVP at 1.75 µM) reduces pY[397]FAK abundance and disrupts ciliary band formation. (C) Blocking FAK phosphorylation (PF573 at 10 µM) reduces pY[397]FAK abundance and disrupts ciliary band formation. (D) Blocking Eph kinase or FAK phosphorylation (as above) significantly reduces the extent of apical constriction in ciliary band cells. Embryos were exposed to inhibitors at 48 hours and apical surface area was quantified at 72 hours. Control embryos (DMSO) form discrete ciliary band regions with apically constricted cells. Addition of NVP (center bar) or PF573 (right bar) results in inhibition of apical constriction, indicating a role for the Eph kinase activity and the FAK activity. Control, *n*=670 cells in ten embryos; Eph inhibitor, *n*=582 cells in ten embryos; FAK inhibitor, *n*=760 cells in 13 embryos. Scale bars: 10 µm.

adjuvant (Sigma) for booster immunizations at a 1:1 ratio. Animals were immunized and housed at the University of Victoria Animal Care Facility. Immunization by subcutaneous injection included 100 µg antigen in 250 µl total volume at 0 days, 21 days and 42 days. A terminal bleed by cardiac puncture was performed at 52-56 days. Blood samples were incubated for 45 minutes at 37°C and placed at 4°C overnight. Clots were centrifuged at 1000 ***g***, serum collected and sodium azide (Sigma) added to a final concentration of 0.02% w/v. Antibody specificity was confirmed by western blotting against the antigen and subsequently against an embryonic lysate. Anti-Sp-Ephrin mouse serum recognized a doublet typical of Ephrin antibody at 38 and 42 kDa, corresponding to the approximate molecular mass of native Ephrin protein. Mice were then used to produce an Sp-Ephrin monoclonal antibody (4D2) according to previous methods (Loveless et al., 2011) and this recognizes bands at ~38 and 42 kDa. Anti-Sp-Eph rat serum recognizes a single band at ~110 kDa, corresponding to the predicted molecular mass of native Sp-Eph protein. All animal experiments were performed according to approved guidelines.

Immunofluorescence microscopy

S. purpuratus embryos were fixed for 5 minutes in PEM buffer (Vielkind and Swierenga, 1989) or ice-cold methanol. Embryos were washed with PBS and probed with primary antibody diluted in SuperBlock (Thermo). Primary antibodies: atypical protein kinase C ζ (aPKC, 1:300, Santa Cruz), Sp-Ephrin (1:2, 4D2 supernatant), Sp-Eph (1:500, serum), Sp-Hnf6 (Yaguchi et al., 2010) (1:700, serum), pY[397]FAK (1:2000, Invitrogen), pY[379]Eph (1:3000, Abcam), Phalloidin-Alexa Fluor 633 (1:300, Invitrogen), pS[19]myosin light chain II (pS[19]MLC, 1:200, Cell Signaling Technology). Embryos were washed three times with PBS and visualized with Alexa Fluor secondary antibodies (Invitrogen) on a Zeiss 700 LSM (Carl Zeiss) confocal microscope.

The contribution of cell division to apical constriction in ciliary band ectoderm was assessed by adding DMSO or 0.6 µM aphidicolin (Sigma, A0781) with 1 µM EdU to sea water at 60 hours. Following fixation, EdU incorporation was detected using a Click-IT detection kit (Life Technologies, C10340) according to manufacturer's direction.

All immunofluorescence images are maximum intensity projections of whole mounted, sea urchin larvae oriented with oral ectoderm at the top and aboral ectoderm at the bottom. Cells shown in the insets were chosen randomly in an area of ciliary band ectoderm or chosen to highlight typical defects observed with treatments. Images used for data analyses were maximum intensity projections that extended from the cell surface to a 3-4 µm depth for cell shape (anti-aPKC) and 7 µm for all cytoskeleton (pSer[19]myosin and Phalloidin). Optimal gain, pinhole diameter and laser intensity settings were established for each antibody/fluorophore combination and settings were re-used consistently. Imaging and analysis was conducted using ZEN software (Carl Zeiss). Adobe Photoshop was used for cropping and assembling figures and to adjust image contrast and brightness.

Cell surface area calculations

For surface area measurements, anti-aPKC was used to visualize apical cell membranes, and ciliary band cells were identified using the ciliary-band-specific marker, anti-Hnf6. Apical membranes were outlined and cell surface area was calculated using ZEN software. Surface area values were exported to Microsoft Excel for further analysis.

Relative intensity measurements

Images were quantified using ZEN software and areas of interest selected by encircling them (when comparing intensity in ciliary band and aboral ectoderm) or by drawing a 5 pixel width line along the structure of interest (when comparing latitudinal and longitudinal expression). Dark pixels and saturated pixels were excluded in relative intensity measurements. Data sets were collected as intensity values per pixel within or along the region of interest and exported into Microsoft Excel for further analysis.

Statistical analyses

Grouped data were analyzed using a one-way ANOVA and the *P*-value for each comparison is reported. A *P*-value below 0.05 was considered statistically significant.

Protein affinity

Ectodermal cells were isolated from embryos at 72 hours (McClay and Marchase, 1979) for preparation of ectodermal cell lysate. Lysate was clarified by ultracentrifugation (4°C, 10 minutes, 100,000 ***g***) and protein quantified by Bradford analysis. Full-length Sp-Eph and the cytoplasmic portion (aa 322-762) of a kinase-dead Sp-Eph, SpEphKD[K445R], were cloned into pGEX4T-1 to create GST fusions and transformed into *E. coli* BL21 for expression using standard protocols. Cells were harvested by centrifugation (4°C, 15 minutes, 12,000 ***g***), resuspended in ice-cold lysis buffer [25 mM Tris-HCl pH 7.6, 150 mM NaCl, 1 mM EDTA, 1% v/v Triton X-100, 5% v/v glycerol, 0.03% w/v SDS, 1 mM dithiothreitol (DTT), 1 mM NaF, 1 mM sodium orthovanadate, 1 mM phenylmethanesulfonyl fluoride (PMSF), 8 µM leupeptin, 1.5 µM pepstatin, 0.3 µM aprotinin)] and lysed by sonication at 4°C. Lysate was clarified by ultracentrifugation (4°C, 10 minutes, 100,000 ***g***) and protein was quantified by Bradford analysis. Fusion protein lysate was incubated for 30 minutes at 4°C with glutathione-agarose at a rate of 35 mg/ml wet resin. Resin was washed with three volumes lysis buffer and ectodermal lysate was added at 35 mg/ml wet

Development (2014) doi:10.1242/dev.100123

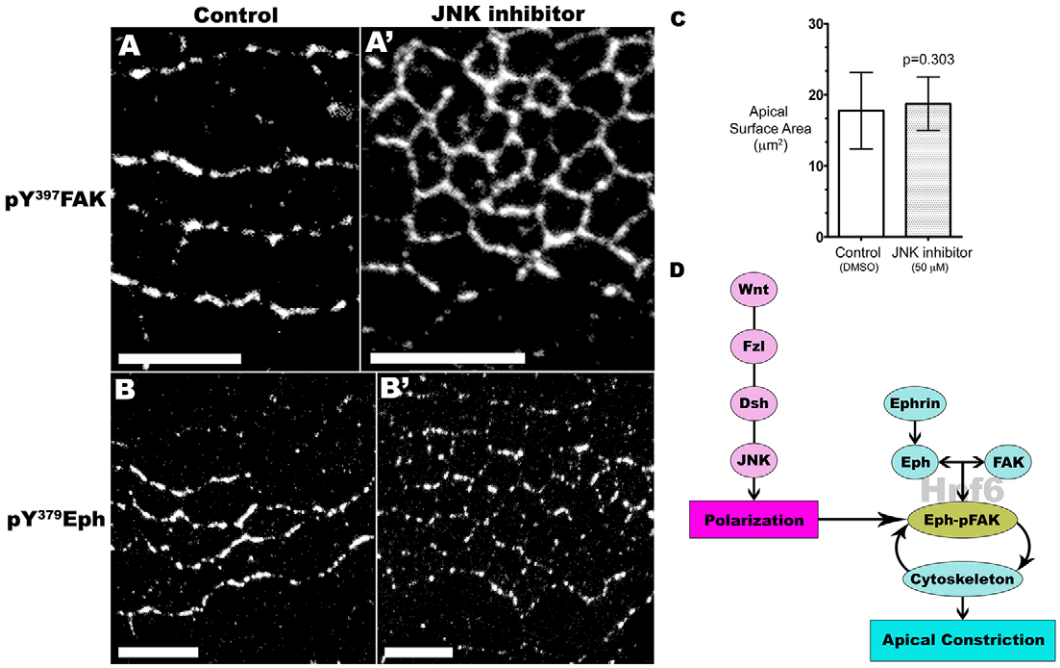

Fig. 9. Planar polarization of ciliary band cells is controlled by the non-canonical Wnt pathway and is dissociable from apical constriction. (A,B) At 72 hours polarization of pY^{397}FAK and pY^{379}Eph at latitudinal apical junctions is apparent in control embryos. (A′,B′) Addition of a JNK inhibitor (50 μM) causes an apparent loss of latitudinal accumulation of pY^{397}FAK and pY^{379}Eph in the ciliary band. (C) Apical constriction is dissociable from planar polarization. Addition of JNK inhibitor at 48 hours does not significantly alter apical surface area of ciliary band cells at 72 hours. (D) Proposed model illustrating parallel, interacting pathways that define apical constriction and formation of a tightly organized ciliary band in sea urchin embryos. Hnf6 provides a permissive environment for Eph-Ephrin signaling leading to formation and accumulation of an Sp-Eph-FAK complex accompanied by cytoskeletal reorganization and apical constriction. The Sp-Eph-FAK complex is planar polarized through the non-canonical Wnt pathway and this polarization pathway is not necessary for apical constriction. Arrows indicate steps in the pathways for which we have provided evidence. Scale bars: 10 μm.

beads and incubated at 4°C for 1 hour with rocking. Beads were washed with three volumes of lysis buffer and proteins eluted with two 0.5 volume additions of elution buffer (5 mM reduced glutathione, 50 mM Tris-HCl, pH 9.0).

SDS-PAGE used 12% polyacrylamide resolving gels with 5% stacking gel in Mini-protean TetraCell (Bio-Rad) for 50 minutes at 200 V in standard running buffer. Proteins were blotted onto polyvinylidene fluoride (PVDF) membrane in standard transfer buffer for 1 hour using Genie Blotter (Idea Scientific). Blots were probed with anti-GST (1:5000, Cedarlane) and anti-pFAK[pY^{397}] (1:1000, Invitrogen). Infrared detection of secondary antibodies (Rockland) was done on an Odyssey Imager (Li-Cor Biosciences) and images were adjusted for brightness and contrast using Photoshop.

Acknowledgements

We thank John H. Henson, James A. Coffman and Caroline Cameron for generously providing reagents, advice or access to equipment. We thank Valerie Taylor for technical assistance.

Competing interests

The authors declare no competing financial interests.

Author contributions

O.A.K. developed materials, concepts and approaches, performed experiments, analyzed data and prepared the manuscript. R.D.B. developed concepts and approaches, analyzed data and edited the manuscript.

Funding

This work was supported by a Discovery Grant from the Natural Sciences and Engineering Research Council of Canada [grant number 2413-2009 RGPIN to R.D.B.].

References

Angerer, L. M., Oleksyn, D. W., Logan, C. Y., McClay, D. R., Dale, L. and Angerer, R. C. (2000). A BMP pathway regulates cell fate allocation along the sea urchin animal-vegetal embryonic axis. *Development* **127**, 1105-1114.

Arold, S. T. (2011). How focal adhesion kinase achieves regulation by linking ligand binding, localization and action. *Curr. Opin. Struct. Biol.* **21**, 808-813.

Ben-Tabou de-Leon, S., Su, Y. H., Lin, K. T., Li, E. and Davidson, E. H. (2013). Gene regulatory control in the sea urchin aboral ectoderm: spatial initiation, signaling inputs, and cell fate lockdown. *Dev. Biol.* **374**, 245-254.

Bradham, C. A., Oikonomou, C., Kühn, A., Core, A. B., Modell, J. W., McClay, D. R. and Poustka, A. J. (2009). Chordin is required for neural but not axial development in sea urchin embryos. *Dev. Biol.* **328**, 221-233.

Burke, R. D. (1978). The structure of the nervous system of the pluteus larva of Strongylocentrotus purpuratus. *Cell Tissue Res.* **191**, 233-247.

Burridge, K. and Wennerberg, K. (2004). Rho and Rac take center stage. *Cell* **116**, 167-179.

Carter, N., Nakamoto, T., Hirai, H. and Hunter, T. (2002). EphrinA1-induced cytoskeletal re-organization requires FAK and p130(cas). *Nat. Cell Biol.* **4**, 565-573.

Darie, C. C., Deinhardt, K., Zhang, G., Cardasis, H. S., Chao, M. V. and Neubert, T. A. (2011). Identifying transient protein-protein interactions in EphB2 signaling by blue native PAGE and mass spectrometry. *Proteomics* **11**, 4514-4528.

Duboc, V., Röttinger, E., Besnardeau, L. and Lepage, T. (2004). Nodal and BMP2/4 signaling organizes the oral-aboral axis of the sea urchin embryo. *Dev. Cell.* **6**, 397-410.

Hildebrand, J. D. (2005). Shroom regulates epithelial cell shape via the apical positioning of an actomyosin network. *J. Cell Sci.* **118**, 5191-5203.

Klein, R. (2012). Eph/ephrin signalling during development. *Development* **139**, 4105-4109.

Krupke, O. A., Yaguchi, S., Yaguchi, Y. and Burke, R. D. (2014). Imaging neural development in embryonic and larval sea urchins. In *Developmental Biology of the Sea Urchin and Other Marine Invertebrates. (Methods in Molecular Biology)*, Vol. 1128 (ed. D. J. Carroll and S. A. Stricker). New York, USA: Humana Press, Springer (in press).

Lapraz, F., Besnardeau, L. and Lepage, T. (2009). Patterning of the dorsal-ventral axis in echinoderms: insights into the evolution of the BMP-chordin signaling network. *PLoS Biol.* **7**, e1000248.

Lee, J. Y. and Harland, R. M. (2007). Actomyosin contractility and microtubules drive apical constriction in Xenopus bottle cells. *Dev. Biol.* **311**, 40-52.

Loveless, B. C., Mason, J. W., Sakurai, T., Inoue, N., Razavi, M., Pearson, T. W. and Boulanger, M. J. (2011). Structural characterization and epitope mapping of the glutamic acid/alanine-rich protein from Trypanosoma congolense: defining assembly on the parasite cell surface. *J. Biol. Chem.* **286**, 20658-20665.

Martin, A. C., Kaschube, M. and Wieschaus, E. F. (2009). Pulsed contractions of an actin-myosin network drive apical constriction. *Nature* **457**, 495-499.

McClay, D. R. and Marchase, R. B. (1979). Separation of ectoderm and endoderm from sea urchin pluteus larvae and demonstration of germ layer-specific antigens. *Dev. Biol.* **71**, 289-296.
Miyoshi, H., Satoh, S. K., Yamada, E. and Hamaguchi, Y. (2006). Temporal change in local forces and total force all over the surface of the sea urchin egg during cytokinesis. *Cell Motil. Cytoskeleton* **63**, 208-221.
Moeller, M. L., Shi, Y., Reichardt, L. F. and Ethell, I. M. (2006). EphB receptors regulate dendritic spine morphogenesis through the recruitment/phosphorylation of focal adhesion kinase and RhoA activation. *J. Biol. Chem.* **281**, 1587-1598.
Nagele, R. G. and Lee, H. Y. (1987). Studies on the mechanisms of neurulation in the chick: morphometric analysis of the relationship between regional variations in cell shape and sites of motive force generation. *J. Exp. Zool.* **241**, 197-205.
Nishimura, T., Honda, H. and Takeichi, M. (2012). Planar cell polarity links axes of spatial dynamics in neural-tube closure. *Cell* **149**, 1084-1097.
Ohashi, K., Nagata, K., Maekawa, M., Ishizaki, T., Narumiya, S. and Mizuno, K. (2000). Rho-associated kinase ROCK activates LIM-kinase 1 by phosphorylation at threonine 508 within the activation loop. *J. Biol. Chem.* **275**, 3577-3582.
Otim, O., Amore, G., Minokawa, T., McClay, D. R. and Davidson, E. H. (2004). SpHnf6, a transcription factor that executes multiple functions in sea urchin embryogenesis. *Dev. Biol.* **273**, 226-243.
Parri, M., Buricchi, F., Giannoni, E., Grimaldi, G., Mello, T., Raugei, G., Ramponi, G. and Chiarugi, P. (2007). EphrinA1 activates a Src/focal adhesion kinase-mediated motility response leading to rho-dependent actino/myosin contractility. *J. Biol. Chem.* **282**, 19619-19628.
Pilot, F. and Lecuit, T. (2005). Compartmentalized morphogenesis in epithelia: from cell to tissue shape. *Dev. Dyn.* **232**, 685-694.
Poustka, A. J., Kühn, A., Radosavljevic, V., Wellenreuther, R., Lehrach, H. and Panopoulou, G. (2004). On the origin of the chordate central nervous system: expression of onecut in the sea urchin embryo. *Evol. Dev.* **6**, 227-236.
Range, R. C., Angerer, R. C. and Angerer, L. M. (2013). Integration of canonical and noncanonical Wnt signaling pathways patterns the neuroectoderm along the anterior-posterior axis of sea urchin embryos. *PLoS Biol.* **11**, e1001467.
Roh-Johnson, M., Shemer, G., Higgins, C. D., McClellan, J. H., Werts, A. D., Tulu, U. S., Gao, L., Betzig, E., Kiehart, D. P. and Goldstein, B. (2012). Triggering a cell shape change by exploiting preexisting actomyosin contractions. *Science* **335**, 1232-1235.
Roose, J. P., Mollenauer, M., Gupta, V. A., Stone, J. and Weiss, A. (2005). A diacylglycerol-protein kinase C-RasGRP1 pathway directs Ras activation upon antigen receptor stimulation of T cells. *Mol. Cell. Biol.* **25**, 4426-4441.
Saudemont, A., Haillot, E., Mekpoh, F., Bessodes, N., Quirin, M., Lapraz, F., Duboc, V., Röttinger, E., Range, R., Oisel, A. et al. (2010). Ancestral regulatory circuits governing ectoderm patterning downstream of Nodal and BMP2/4 revealed by gene regulatory network analysis in an echinoderm. *PLoS Genet.* **6**, e1001259.
Sawyer, J. M., Harrell, J. R., Shemer, G., Sullivan-Brown, J., Roh-Johnson, M. and Goldstein, B. (2010). Apical constriction: a cell shape change that can drive morphogenesis. *Dev. Biol.* **341**, 5-19.
Shi, Y., Pontrello, C. G., DeFea, K. A., Reichardt, L. F. and Ethell, I. M. (2009). Focal adhesion kinase acts downstream of EphB receptors to maintain mature dendritic spines by regulating cofilin activity. *J. Neurosci.* **29**, 8129-8142.
Slack-Davis, J. K., Martin, K. H., Tilghman, R. W., Iwanicki, M., Ung, E. J., Autry, C., Luzzio, M. J., Cooper, B., Kath, J. C., Roberts, W. G. and Parsons, J. T. (2007). Cellular characterization of a novel focal adhesion kinase inhibitor. *J. Biol. Chem.* **282**, 14845-14852.
Strathmann, R. R. (1971). The feeding behavior of planktonic echinoderm larvae:mechanisms, regulation, and rates of suspension-feeding. *J. Exp. Mar. Biol. Ecol.* **6**, 109-160.
Strathmann, R. R. (2007). Time and extent of ciliary response to particles in a non-filtering feeding mechanism. *Biol. Bull.* **212**, 93-103.
Strathmann, R. R., Jahn, T. L. and Fonseca, J. R. C. (1972). Suspension feeding by marine invertebrate larvae: clearance of particles from suspension by ciliated bands of a rotifer, pluteus, and trochophore. *Biol. Bull.* **142**, 505-519.
Sweeton, D., Parks, S., Costa, M. and Wieschaus, E. (1991). Gastrulation in Drosophila: the formation of the ventral furrow and posterior midgut invaginations. *Development* **112**, 775-789.
Thomas, J. W., Ellis, B., Boerner, R. J., Knight, W. B., White, G. C., II and Schaller, M. D. (1998). SH2- and SH3-mediated interactions between focal adhesion kinase and Src. *J. Biol. Chem.* **273**, 577-583.
Tilghman, R. W. and Parsons, J. T. (2008). Focal adhesion kinase as a regulator of cell tension in the progression of cancer. *Semin. Cancer Biol.* **18**, 45-52.
Uehara R., Hosoya, H. and Mabuchi, I. (2008). In vivo phosphorylation of regulatory light chain of myosin II in sea urchin eggs and its role in controlling myosin localization and function during cytokinesis. *Cell Motil. Cytoskeleton* **65**, 100-115.
Vielkind, U. and Swierenga, S. H. (1989). A simple fixation procedure for immunofluorescent detection of different cytoskeletal components within the same cell. *Histochemistry* **91**, 81-88.
Wilkinson, D. G. (2000). Eph receptors and ephrins: regulators of guidance and assembly. *Int. Rev. Cytol.* **196**, 177-244.
Yaguchi, S., Yaguchi, J., Angerer, R. C., Angerer, L. M. and Burke, R. D. (2010). TGFβ signaling positions the ciliary band and patterns neurons in the sea urchin embryo. *Dev. Biol.* **347**, 71-81.